F. Aylin (Sungur) Konuklar · Viktorya Aviyente
Taner Zafer Sen · Ivet Bahar

Modeling the deamidation of asparagine residues via succinimide intermediates

Abstract Density functional theory (B3LYP/6-31G*) has been used to study the cyclization, deamidation and hydrolysis reactions of a model peptide. Single point energy calculations with the polarized continuum model drastically lower the activation energy for cyclization in a basic medium. Confirmation of the experimental results that cyclization is slower than deamidation in acidic media and the opposite is true in basic media has enabled us to propose mechanisms for both processes.

Keywords Deamidation · Succinimide · Density functional theory · Hydrolysis of peptides

Introduction

Spontaneous reactions such as deamidation, isomerization and racemization that affect the structure and function of proteins sometimes lead to their degradation. Deamidation is the cleavage of the amide group from the backbone of the amino acid residue, isomerizationis the transfer of the backbone group to the side-chain, and finally racemization is a change of configuration of the α-carbon of the residue. Non-enzymatic deamidation of asparagine (Asn) and glutamine (Gln) residues in peptides and proteins is a well-known phenomenon, which may occur under physiological conditions. [1, 2, 3] At high pH values, hydrolysis of amide bonds is accelerated whereas at neutral pH values, especially when Asn is followed by a glycine (Gly) residue, significant reaction rates have been observed. [4, 5] The deamidation reaction mechanism involves the formation of a five-membered cyclic imide intermediate undergoing subsequent hydrolytic ringopening to give L-aspartic acid (Asp) and L-isoaspartic acid (Iso-

Asp) in a ratio of 1:3. [6] In addition, small amounts of D-aspartic acid and D-isoaspartic acid were observed, indicating slow racemization of the cyclic imide.

Spontaneous deamidation through the cyclization mechanism has been implicated in the inactivation of a number of enzymes. [7] The deamidation reaction has a much shorter half-life than that for peptide bond hydrolysis, varying from days to weeks depending on the amino acid sequence. [3] Antibodies that catalyze the deamidation and β-aspartyl shift of modified asparaginyl–glycyl dipeptides have been reported. [8] Two classes of antibodies that control theisoaspartate to aspartate product ratio were generated. One class catalyzes only the hydrolysis of succinimide and the other catalyzes both the rate-limiting deamidation and the subsequent succinimide hydrolysis. [8] In the uncatalyzedreaction for the synthetic peptide Ac–Asn–Gly–Phen, the product has an isoaspartate to aspartate ratio of 3.6. [9] Liotta et al. [9] have found that the half-life for the spontaneous succinimide cyclization reaction without any catalysis by antibody is ~4.7 days whereas the antibodies reduce it to ~1.6 h.

The formation of the succinimide ring may occur not only in vivo but also during the purification, storage and manipulation of peptides and proteins. [10] The reduction in biological activity of growth hormone-releasing factors that have been stored in solution for an extended period of time has been ascribed to a deamidation process via succinimide. [11] The deamidation reaction also takes place in triosephoshate isomerase (TIM), an enzyme that rapidly and reversibly converts dihydroxyacetonephosphate (DHAP) into glyceraldehyde-3-phosphate (GAP) in the glycolytic pathway. Sun et al. [12] have shown that two sites on each subunit deamidate and introduce two pairs of negative charges into the subunit interface. These negative charges initiate subunit dissociation and unfolding and lead to proteolytic degradation.

The formation of a succinimide ring at theasparagine residue has been shown to be a multistep process with a change in the rate-determining step at around neutral pH values, [13] the rate of cyclization being proportional to the pH of the medium. [2] In order to obtain a deeper

F. Aylin (Sungur) Konuklar · V. Aviyente (✉)
Department of Chemistry, Bogaziçi University,
80815, Bebek, Istanbul, Turkey
e-mail: aviye@boun.edu.tr

T. Zafer Sen · I. Bahar
Polymer Research Center, Bogaziçi University,
80815, Bebek, Istanbul, Turkey

understanding of the kinetic behavior of this reaction, Capasso et al. [13] studied the formation of the succinimide derivative from the peptide Ac–Gly–Asn–Gly–Gly–NHMe and have proposed a kinetic mechanism that explains the data reported previously. Capasso's experimental results can be rationalized in terms of the reaction pathway depicted in Scheme 1. The asparagine residue (**1**) is in equilibrium with the anionic intermediate (**2**) prior to the intramolecular cyclization to the tetrahedral intermediate (**3**). Proton transfer to the leaving group from a general acid and the concerted breakdown of the tetrahedral intermediate **3** gives the D- and L-succinimide products (**2**). Finally the aspartate and isoaspartate products are obtained by hydrolysis. The most likely rate-determining step in the cyclization reaction has been found to be the decomposition of the tetrahedral intermediate, with the expulsion of ammonia, as suggested by the absence of antibody-catalysis for the cyclization of the methyl ester. [9] At acidic pH, the cyclization to **3** is the rate-determining step and therefore the reaction is specific-base catalyzed, whereas at higher pH the conversion of **3** to **4** becomes the rate-determining step and therefore the reaction is general-acid specific-base catalyzed. Cyclic imide formation according to the mechanism explained above necessitates a significant change in the local protein structure. Therefore Gly and, to a lesser extent Serine (Ser), with their small side chains, are more tolerant of this structural change. The reaction mechanism is also consistent with the fact that Gln residues deamidate more slowly than Asn, since formation of a six-membered cyclic imide is lessfavored entropically.

Recently, kinetic evidence has indicated that peptide bond cleavage on an Asn–Sar-containing peptide is a multi-step process with a change in the rate-determining step at pH=8.5–9.0. At pH<8.5, the formation of cyclic intermediate is rate determining, whereas at higher pH it is the departure of the leaving group. [14]

In another study, it has been shown that the succinimide ring-formation leads to protein splicing, [15] during which a C terminal succinimide is one order of magnitude more stable than the internal succinimide. [16]

Computationally, ab initio (RHF/6–31+G*) and density functional (B3LYP/6–31+G*) theories have been used to identify the factors that lead to enhanced succinimide α-carbon acidity and racemization quantitatively. [17]
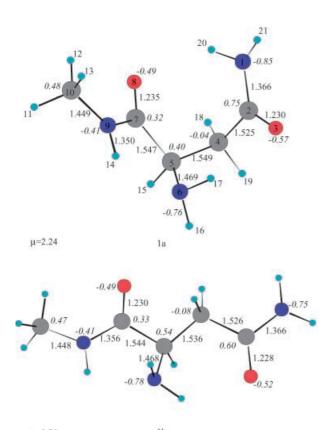
In this study we have modeled the scheme proposed by Capasso et al. (Scheme 1) [13] using density functional theory (B3LYP/6-31G*).The X and Y groups in Scheme 1 have been chosen as hydrogen in order to save computer time. The effect of a polar environment on the energetics of the cyclization, deamidation and hydrolysis of the model peptide has also been considered.
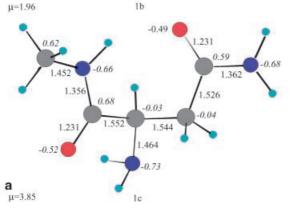
Methodology

Ab initio molecular orbital calculations employed the Gaussian 94 program. [18] To find the most stable structures of the reactants and intermediates, free rotation

Table 1 Calculated energies (a.u.) (B3LYP/6-31G*) for the compounds shown in Figure 1. Electronic energies are in the first column, energies with zero point correction are in the second column, and total energies are in the last column. Energies in solution are given in parentheses in italics
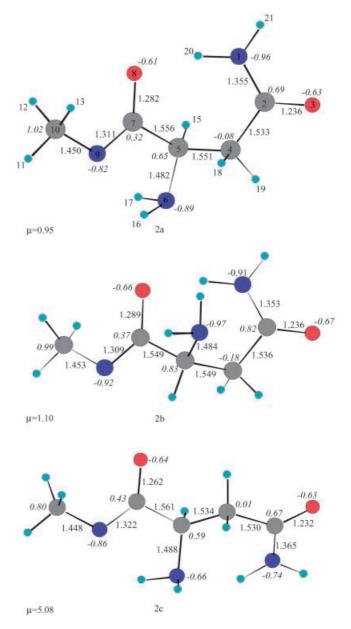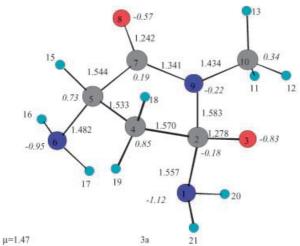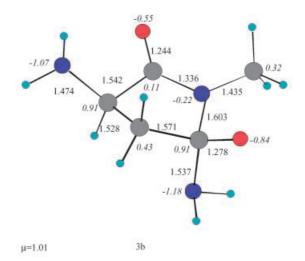
	Energy (solvent)	Energy+ZPE	Energy+ZPE+thermal
1a	–511.891468 (*–511.909396*)	–511.713091	–511.702097
1b	–511.887556	–511.710548	–511.698940
1c	–511.886177	–511.709472	–511.697621
2a	–511.308040 (*–511.398733*)	–511.145212	–511.134363
2b	–511.305516	–511.142797	–511.131847
2c	–511.300483	–511.137668	–511.126673
TS23a	–511.274478 (*–511.383180*)	–511.111886	–511.101771
TS23b	–511.274605 (*–511.383088*)	–511.111798	–511.101921
3a	–511.279882 (*–511.383463*)	–511.115891	–511.105845
3b	–511.277936 (*–511.383318*)	–511.114491	–511.104180
TS13a	–511.806042 (*–511.833668*)	–511.632469	–511.621940
TS13b	–511.800387 (*–511.834784*)	–511.625789	–511.615330
3a+H	–511.859371 (*–511.881182*)	–511.681015	–511.670696
3b+H	–511.858785 (*–511.883928*)	–511681024	–511.670425
TS34a	–511.800288 (*–511.824443*)	–511.628343	–511.617802
TS34b	–511.803586 (*–511.830681*)	–511.631514	–511.621033
4L	–455.325151 (*–455.343128*)	–455.187321	–455.178356
4D	–455.325091 (*–455.343161*)	–455.187241	–455.178290
TS45L	–531.665253 (*–531.681326*)	–531.506373	–531.496140
TS45D	–531.663227 (*–531.680968*)	–531.504644	–531.494324
TS46L	–531.662443 (*–531.680741*)	–531.504177	–531.493644
TS46D	–531.660841 (*–531.678335*)	–531.502142	–531.491700
5a	–531.751788 (*–531.774723*)	–531.586723	–531.575528
5b	–531.742791	–531.578376	–531.567024
5c	–531.746886	–531.582084	–531.570788
6a	–531.754918 (*–531.778110*)	–531.589942	–531.578857
6b	–531.752785	–531.587976	–531.576690
NH$_3$	–56.547948 (*–56.554618*)	–56.513415	–56.510557
H$_2$O	–76.408953 (*–76.418302*)	–76.387784	–76.384960
OH$^-$	–75.720733 (*–75.895160*)	–75.712954	–75.710633

Fig. 1 a Optimized structures (B3LYP/6-31G*) for compounds **1** and **2**. **b** Optimized structures (B3LYP/6-31G*) for compounds **3**, **3**+H+ and **4**.**c** Optimized structures (B3LYP/6-31G*) for compounds **5** and **6**. **d** Optimized structures (B3LYP/6-31G*) for compounds **TS13**, **TS23** and **TS34**. **e** Optimized structures (B3LYP/6-31G*) for compounds **TS45(D)**, **TS45(L)**, **TS46(D)** and **TS46(L)**. **f** Optimized structures (PM3) for compounds Precomplex* and **TS12***
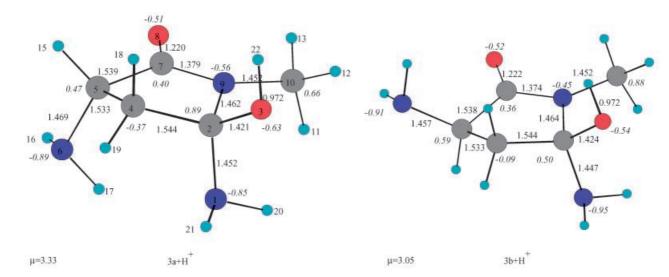
around all single bonds has been performed with the MM2 force field in Spartan. [19] The conformers with minimum energy have been optimized further with AM1. The optimized AM1 geometries were used to initiate searches for the optimized B3LYP/6-31G* geometries. The charges have been calculated by using the CHELP option in the Gaussian 94 program. Each minimum energy structure was verified by its all real harmonic vibrational frequencies. Transition states between reactant and products were located with AM1 by using
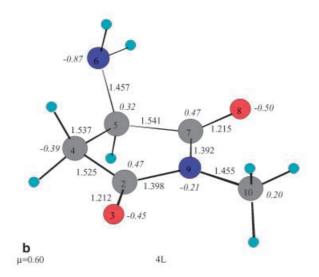
the Linear Synchronous Transit (LST) option in Spartan. The optimized transition state structures were further optimized with B3LYP/6-31G* and characterized by a single imaginary frequency belonging to the critical bonds. Zero point (ZPE) and thermal energies were added to the electronic energy in order to evaluate the activation barriers at 25 °C. The calculated energies (a.u.) (B3LYP/6-31G*) of the compounds displayed in Figure 1a–e are gathered in Table 1. In Figure 1a–e, the compounds are denoted as *n*a, *n*b, *n*c where *n* is number of the compound in the reaction path and a, b, c show the different conformers in order of increasing energy. The transition states are denoted as TS*nn′* where *n* is the reactant and *n′* is the product of the path investigated. Figure 1f shows the transition structure TS12 between 1 and 2 and its corresponding precomplex optimized with the semiempirical PM3 method. [20] In Figure 2a–f, the reaction paths (1→2, 1→3, 2→3, 3→4, 4→5, 4→6) are shown

150

Fig. 1b Legend see page 149

Fig. 1c Legend see page 149

Table 2 Calculated electronic energies (a.u.) (PM3) for the compounds shown in Figure 2a–g

Compound	Energy [a.u.]
1a	–0.140896
2a	–0.189911
Precomplex	–0.244420
TS12	–0.242662
TS23a	–0.172324
3a	–0.175362
TS13a	–0.068781
3a+H$^+$	–0.146288
TS34a	–0.077008
4D	–0.132445
NH$_3$	–0.004908
H$_2$O	–0.085158
OH$^-$	–0.027897

with their relative energies (kcal mol^{-1}) versus the reaction coordinate. The reaction paths given by PM3 are drawn in Figure 2f and g. The calculated energies (a.u) (PM3) of the compounds shown in Figure 2f and g are displayed in Table 2. The effect of a polar environment on the reaction path proposed by Capasso et al. [13] has been taken into account by carrying out single point energy calculations in water (ε=78.5). The polarized continuum model (PCM), which defines the cavity as the union of a series of interlocking atomic spheres, has been utilized for the solvated reaction paths. [21] In this model, the effect of polarization of the solvent continuum is computed by numerical integration.
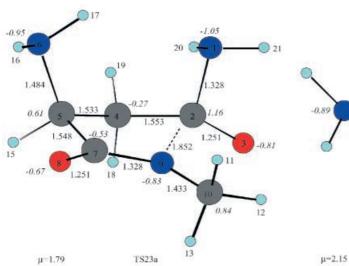
Results and discussion

The compounds shown in Figure 1a–e have been optimized and the energetics for the cyclization, deamidation and hydrolysis reactions evaluated. Compound **1** is the initial peptide, **2** (=1$^-$ in [13]) is the anion in equilibrium with **1**. Structure **3** (=In$^-$ in [13]) is the tetrahedral cyclic intermediate and structure **3**+H$^+$ is the O-protonated compound **3** formed via the cyclization reaction. Compound **4** is 2-methyl-4-aminosuccinimide, **5** and **6** are the isoaspartate and aspartate products formed by the hydrolysis of **4**.
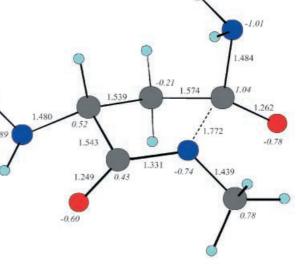
μ=5.92   TS13a

μ=6.72   TS13b

μ=1.79   TS23a

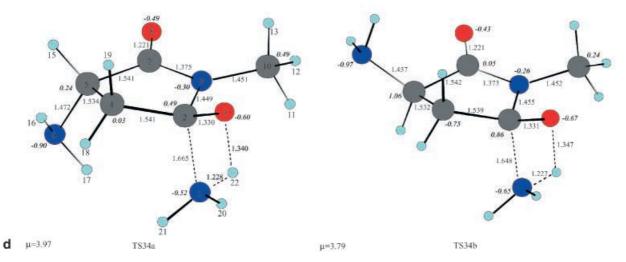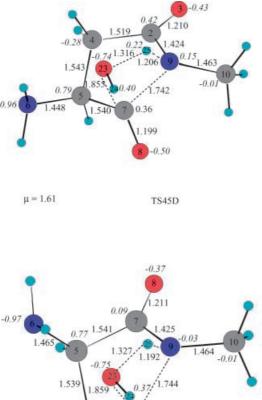μ=2.15   TS23b

d   μ=3.97   TS34a

μ=3.79   TS34b
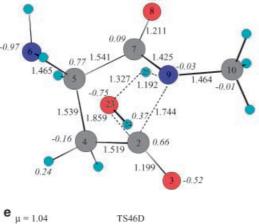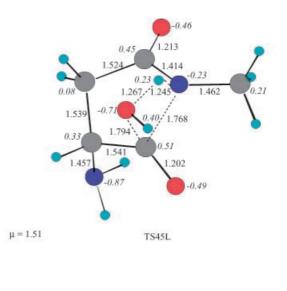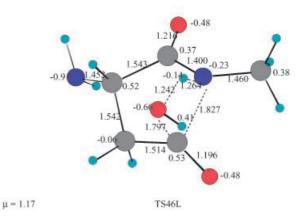
Fig. 1d Legend see page 149
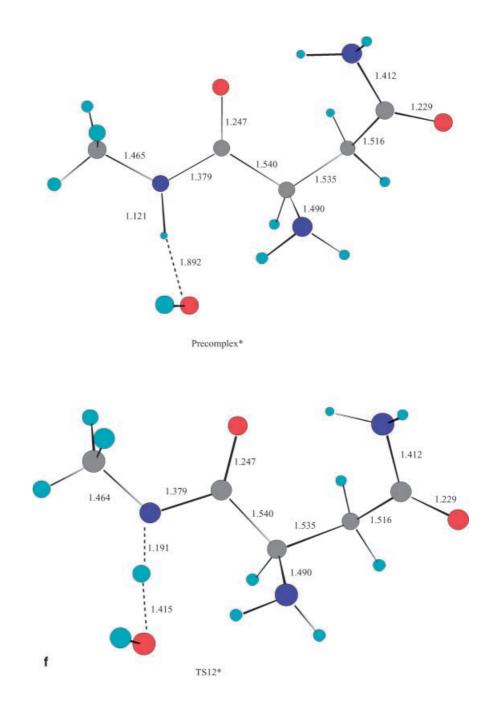
Fig. 1e Legend see page 149

Geometries

Of the three conformers for compound **1**, **1a** has the lowest energy. Its conformational preference is probably due to formation of a ring upon rotation around the C5–C7 bond. The hydrogen bonds O3...H17 (2.304 Å), N6...H14 (2.131 Å) and O8...H20 (2.252 Å) stabilize this structure. The hydrogen atom (H14) that bears the highest positive charge (0.19) will be abstracted in basic solution. The second structure, **1b**, has the lowest dipole moment of the three conformers. It has a quasi-planar structure with two carbonyl groups *anti* to each other, which leads to a reduced dipole moment. The long range interactions N6...H14 (2.132 Å) and O3...H16 (2.271 Å) stabilize this structure. The lone electron pair of N6 is tilted towards H14 in both **1a** and **1b**, the two lowest energy conformers. Although **1a** has a higher dipole moment than **1b**, the stabilizing effect of a hydrogen bond between O8 and H20 in **1a** overcomes the stabilizing effect of the low dipole moment in **1b**. The third structure, **1c**, has the highest dipole and is the highest energy conformer. The stabilization gained by the hydrogen bonds

O8...H16 (2.272 Å) and O3...H14 (1.989 Å) is not sufficient to overcome the destabilization created by its high dipole moment and the steric repulsion between N9 and O3. A similar conformation has been found by Lifson et al. [22] for succinamide.

Compound **2** is formed by a proton loss from N9 in compound **1**. It is interesting to note that the free electron pair is partially localized on oxygen (–0.61) as described by Capasso et al. [13] and partially located between C7 and N9 (1.311 Å), as shown by comparison with the same bond (1.350 Å) in compound **1**. For compound **2**, the lowest dipole moment (0.95 D) belongs to the lowest energy conformer **2a**. The hydrogen bonds O8...H20 (1.671 Å) and N9...H17 (2.182 Å) also stabilize **2a** and lower its energy. The last structure **2c** is the highest energy conformer and has the highest dipole moment because of two parallel carbonyl oxygens and the lone electron pair on nitrogen. The long range stabilizing interactions, O8...H20 (1.680 Å) and O8...H16 (2.430 Å) in **2b**, and N6...H20 (1.928 Å) and N9...H17 (2.147 Å) in **2c**, were not sufficient to overcome the destabilizing effect produced by the high dipole moment. Note the difference in the C–N bond lengths for the amide bond C7–N9 (1.311 Å in **2a**) and the terminal C2–N1 bond (1.355 Å in **2a**). The C–N bond in the amide moiety is

Fig. 1f Legend see page 149
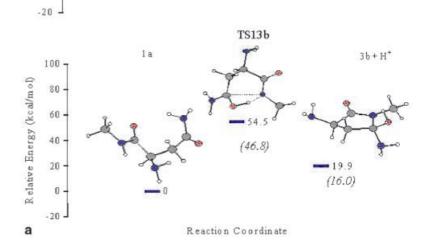

Precomplex*

f

TS12*

shorter than the C2–N1 bond, confirming the delocalization of electrons toward the C–N amide bond. The lone electron pair on N9 (–0.82) can readily attack the positively charged C2 (0.62) in order to form a cyclic compound. After deprotonation of compound **1**, the charge distribution changes drastically. The charge on O8 (–0.49 in **1a**) becomes –0.61 in **2a**. After deprotonation of compound **1a**, the negative charge on N9 (–0.41 in **1a**) doubles in the case of **2a**. The C5–N6 bond in **2a** is lengthened by 0.02 Å relative to the protonated structure and has a value of 1.482 Å.

TS13 is the transition state for the neutral cyclization reaction. It forms via cyclization of compound **1**. The product of this reaction is **3**+H⁺, which is the O-protonated tetrahedral cyclic intermediate. **TS13** is a four-membered tetrahedral quasi-planar transition state [23] and it involves a concerted proton transfer mechanism. A similar transition state was proposed by Coll et al. for the hydrolysis of a pyrazolidinone ring. The reaction is endothermic and the transition state is product-like. The –NH$_2$ group can be *syn* (**TS13a**) or *anti* (**TS13b**) to the –OH group. **TS13a** is the lowest energy conformer and also has a lower dipole moment than **TS13b**. The N9C2O3H14 dihedral angle is 8° in **TS13a** and 17° in **TS13b**. The C2O3 bond is 1.331 Å, between a single and a double bond and the H14O3 bond length is 1.02 Å, indicating a late transition state.

The transition state **TS23** is formed in such a way that the lone electron pair on N9 (in compound 2) has attacked C2. The –NH$_2$ groups can be *syn* (**TS23a**) or *anti*

Fig. 2 a Energy profile for neutral cyclization of **1** to **3**+H⁺. **b** Energy profile for anionic cyclization of **2** to **3**. **c** Energy profile for deamidation of **3** to **4**. **d** Energy profile for hydrolysis of **4** to **5**. **e** Energy profile for hydrolysis of **4** to **6**. **f** Energy profiles for deprotonation of **1*** to **2***, neutral cyclization of **1*** to **3**+H⁺*. **g** Energy profiles for anionic cyclization of **2*** to **3***, deamidation of **3*** to **4***

Fig. 2b

Fig. 2c Legend see page 155

Fig. 2d Legend see page 155

Fig. 2e Legend see page 155

Fig. 2f Legend see page 155

Fig. 2g Legend see page 155

g   Reaction Coordinate

(**TS23b**) to the –OH group. The transition state resembles the product more than the reactant since the cyclization is endothermic. **TS23** is expected to be a late transition state according to the Hammond postulate. The N9...C2 distances for **TS23a** (1.852 Å) and **TS23b** (1.772 Å) are 1.583 Å and 1.603 Å, respectively, in compound **3a** and **3b**, confirming the Hammond postulate. The difference between the two conformers **TS23a** (*syn*-NH$_2$) **TS23b** (*anti*-NH$_2$) is only 0.0094 kcal mol^{-1}, the two conformers can be considered to be isoenergetic. The possible long-range interac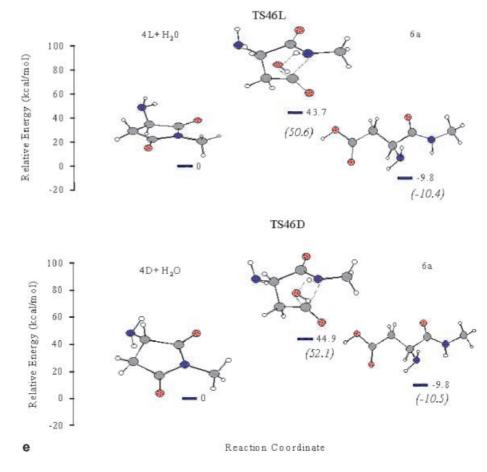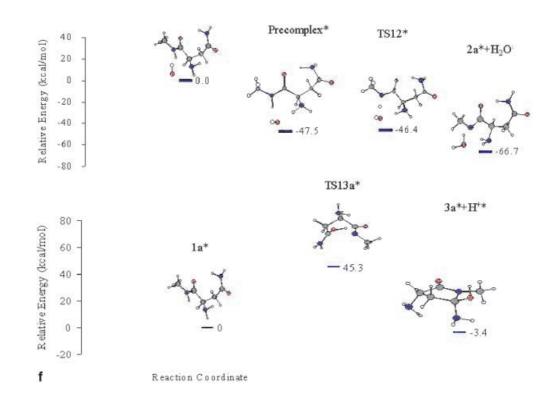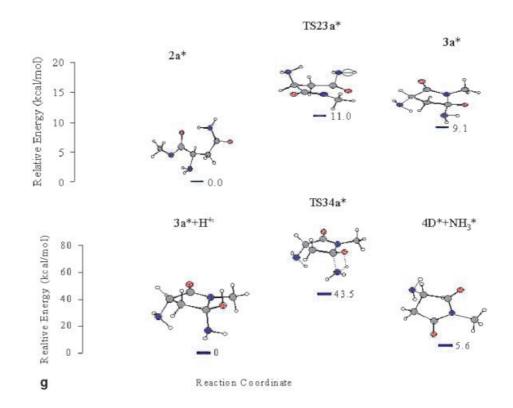tions, which stabilize structure **TS23**, are H20...N9 (2.375 Å), H17...N1 (2.509 Å), H16...O8 (2.579 Å) and H21...O3 (2.292 Å). Compound **3**, is formed via the cyclization of compound **2** through the late transition state **TS23**. There are two possible structures for compound **3**, either the two –NH$_2$ groups are *syn* to each other with respect to the hydroxyl group (**3a**) or they are *anti* to each other (**3b**). The energy difference between the two conformers is 1.04 kcal mol^{-1}. The long-range interactions N1...H17 (2.221 Å), O3...H21 (2.491 Å) and O3...H22 (2.550 Å) stabilize **3a** more than **3b**, in which the N1...H17 interaction is not present.

In order to locate the transition state **TS34** between compound **3** and compound **4**, compound **3** is protonated. For the protonated compound **3**, **3**+H$^+$, the C2–O3 distance becomes 1.421 Å, whereas the C2–N9 becomes 1.462 Å due to a decrease in charge on atom C2 relative to the same atom in compound **3**. The lowest energy conformer is the one with two –NH$_2$ groups *syn* to each other. Hydrogen bonds H21...O8 (2.515 Å), H20...O8 (2.503 Å), H20...N9 (2.647 Å) and H22...N1 (2.531 Å)

stabilize the structure by lowering its energy. In the second conformer, where two NH$_2$ groups are *anti* relative to the ring, the long-range interactions H21...O8 (2.517 Å), H20...O8 (2.505 Å), H22...N1 (2.542 Å) stabilize the structure. The two conformers **3a**+H$^+$ and **3b**+H$^+$ differ by only 0.17 kcal mol^{-1}. In **TS34**, the C2–O3 bond (1.331 Å) is between a CO double (1.221 Å) and a CO single (1.356 Å) bond. The NH$_2$ bonded to C2 abstracts hydrogen from the geminal OH group to eliminate NH$_3$. H22 is almost equally bonded to O3 (~1.340 Å) and N1 (~1.228 Å). The structure in which the two NH$_2$ groups are *anti* (**TS34b**) to each other has the lowest energy. The deamidation reaction is exothermic and the transition state **TS34** resembles the reactant **3** more than product **4**.

In compound **4**, the dihedral angle of the CH$_3$ with respect to the ring is very small (3°), and a unique conformer has been located for this compound; **4D** and **4L** are isoenergetic. In structure **4**, N6 outside the ring is the most negative center (–0.87). The CN distances in the ring are almost identical except that the C7–N9 bond vicinal to the C bearing the NH$_2$ group is slightly shorter (–0.005 Å) than the C2–N9 bond. This is because the electron-donor NH$_2$ group on C5 is closer to C7–N9.

During hydrolysis, H$_2$O approaches compound **4** to cleave either the C7–N9 or the C2–N9 bond to form **5** or **6**, respectively. Depending on the direction of attack of water on compound **4**, two different transition structures **TS45 (D)** and **TS45 (L)** can be located for the formation of compound **5** as well as for compound **6** (**TS46(D)** and **TS46(L)**). In all of these transition states a four-membered ring is formed between the breaking C7–N9 and

O23–H25 and the forming O23–C7 and N9–H25 bonds. The imaginary frequency belongs to these four bonds. **TS45** does not have a planar ring structure and one can distinguish a difference in conformation as well as a difference in energy between compounds **TS45(D)** and **TS45(L)**. The NH_2 group on C5 canbe on either the same or the opposite side as the lone pair on N9. The attack of water on compound **4** occurs in such a way that hydrogen a of H_2O is attracted towards the lone pair on N9 and the OH of water attacks the carbonyl carbon. When H_2O is on the same side as the pending NH_2 group on C5, it forms **TS45(L)** and **TS46(D).** If on the other hand, the attack is from the opposite side, **TS45(D)** and **TS46(L)** will form.

Of the conformers for compound **5**, **5a** is that with the lowest dipole moment. Two possible hydrogen bonds H25...N6 (2.02 Å) and H16...O8 (2.49 Å) lower the energy of **5a**. Structure **5b**, despite its high dipole moment is stabilized by long-range attractive interactions H25...O3 (2.405 Å), H16...O3 (2.248 Å) and H17...O8 (2.500 Å) and is the second lowest energy conformer.

In the last conformer, **5c**, the only possible hydrogen bond is H17...O8 (2.148 Å).

In the case of product **6**, the lowest energy conformer **6a** has the lowest dipole moment and is stabilized by hydrogen bonds H17...O8 (2.415 Å) and H25...N6 (2.146 Å).

Energetics

The energetics for the formation of the succinimide derivative from the peptide are shown in Scheme 1, its deamidation and hydrolysis into isoaspartate and aspartate have been modeled and the barriers for each step are shown in Figure 2a–g. The cyclization of the peptide **1** has been considered in the neutral (**1**→**3**+H^+) and basic forms (**2**→**3**). The cyclization of the neutral peptide proceeds through **TS13a**, whereas the cyclization of the anion **2** takes place via **TS23a**. The cyclization in a basic medium has a barrier of 20.5 kcal mol^{-1}, whereas the neutral form is much slower with a barrier of 50.3 kcal mol^{-1}. In solution, the barrier for the cyclization of the anion drops considerably (9.8 kcal mol^{-1}) as expected from stabilizing interactions between the charged species and a polar environment.

As mentioned earlier by Capasso et al. [13] (Scheme 1), at acidic pH the cyclization to compound **3** is rate determining, whereas at higher pH the conversion of compound **3** to compound **4** becomes rate limiting. This experimental result can be rationalized by comparing the barriers for the cyclization (**1** to **3**+H^+) and the deamidation (**3**+H^+ to **4**) in the neutral form and in basic solution (**2** to **3** and **3** to **4**), respectively. According to the reaction barriers displayed in Figure 2, in the neutral form the cyclization is slower (E_a=50.3 kcal mol^{-1}) than deamidation (E_a=31.0 kcal mol^{-1}) and the rate of the reaction is determined by the cyclization process. In basic medium, the barrier from **3** to **4** has been calculated by

balancing the conversion from **3** to **4**, thus adding H_2O to compound **3** and OH$^-$ to **4**. This calculation shows that the cyclization requires 20.5 kcal mol^{-1}, whereas deamidation in basic medium needs 99.9 kcal mol^{-1}.

These computational results show that the rate-determining step varies according to the medium. The same analysis has been carried out in solution with single point calculations. The cyclization of the neutral compound (**1**) requires 47.5 kcal mol^{-1}, whereas the deamidation reaction in the same medium demands 31.7 kcal mol^{-1}. In solution, the barrier for the cyclization reaction for the basic medium (**2**→**3**) is 9.8 kcal mol^{-1}, whereas the barrier for the deamidation reaction (**3**→**4**) is 47.6 kcal mol^{-1}. Our results in the gas phase and in solution confirm that the deamidation is the rate-determining step in basic media, as suggested by Capasso et al. [13]

Nevertheless, our previous discussion of the reaction in basic media does not include the deprotonation of the model peptide (**1**), since we were unable to locate a transition structure between compounds **1** and **2** with B3LYP/6-31G*. Recently, high level ab initio and density functional theory molecular orbital calculations have been used to investigate the physical properties of a model low barrier hydrogen bond system. The hydrogen bond formed was found to be extraordinarily short and strong (27 kcal mol^{-1}) at B3LYP/6-31++G(d,p) with an enthalpy of activation that is less than the zero point vibrational energy of the system. [24] Since the barrier for deprotonation is extremely low, the discussion of the rate-determining step in basic medium does not lose its validity. However, we have located the transition structure **TS12** with the PM3 method (Figure 1f). In order to discuss the energetics of the reactions involved in Scheme 1 with confidence, we have reproduced the cyclization and deamidation paths in both neutral and basic media with the same method. B3LYP/6-31G* calculations have indicated the deprotonation (**1**→**2**) reaction to be highly exothermic (66.9 kcal mol^{-1}) and the corresponding transition state **TS12** was expected to be early. As seen from Figure 2f, a precomplex much lower in energy than the reactants is formed and the activation barrier is 1.1 kcal mol^{-1}. The cyclization reaction of the anion (**2**) to cyclic intermediate (**3**) requires only 11.0 kcal mol^{-1}, whereas the deamidation reaction in basic media needs 97.6 kcal mol^{-1} (Figure 2g). In neutral media PM3 predicts the cyclization step (E_a=45.3 kcal mol^{-1}) to be slower than the deamidation reaction (E_a=43.5 kcal mol^{-1}) as predicted by B3LYP/6-31G*. These findings support the usage of PM3 in the discussion of the deprotonation reaction (**1**→**2**). Deprotonation is highly exothermic (66.7 kcal mol^{-1} with PM3 and 66.9 kcal mol^{-1} with B3LYP/6-31G*). Thus, neither the deprotonation path nor the cyclization reaction can be rate determining in basic media. The former has a low barrier and the latter has excess energy liberated during the deprotonation reaction.

Another experimental finding, which has been reproduced computationally, is Wright's [25] finding that, in

contrast to the long half-life required for the peptide bond hydrolysis, the deamidation has a much shorter half-life. As seen from Figure 2d–e, the barrier for hydrolysis ($4\rightarrow5$ or $4\rightarrow6$) is almost 10 kcal mol^{-1} higher than that for deamidation ($3\rightarrow4$) in the neutral form.

The rate constants for the reactions have been calculated by using an Arrhenius-type expression assuming the same value for the pre-exponential factor for every enantiomer. The temperature is taken as 25 °C. The calculated ratio $k_{45(D)}/k_{46(L)}$ is 1.96 in the gas phase. Capasso et al. [6] have claimed that the hydrolysis of succinimide canoccur on either side of the imide nitrogen, thus generating two compounds, aspartate and isoaspartate in approximately 1:3 ratio. Thus, our (B3LYP/6-31G*) calculations mimic qualitatively the experimental findings.

Conclusions

In this paper we have presented results from density functional theory (B3LYP/6-31G*) calculations of a model peptide. In basic media the deamidation process has a higher activation barrier than the cyclization step, in agreement with experimental findings. Calculations on the hydrolysis of two amide bonds have reproduced the relative experimental abundance (1:3) [6] of the aspartate versus the isoaspartate product qualitatively (1:1.96). PM3 has been used to locate the transition structure for the deprotonation of the model peptide. The deprotonation of the model peptide analyzed with PM3 has also confirmed the deamidation path to be rate determining with this method as well. Reproduction of the experimental results suggests that the geometries located for transition structures are plausible geometries along the cyclization, deamidation and hydrolysis reaction paths of the model peptide. Similar transition states can be located to reproduce the kinetics as well as the distribution of products for peptides with longer chains.

References

1. Robinson, A. B.; Rudd, C. *Curr. Top. Cell Regul.* **1974**, *8*, 248.
2. Wright, H. T. *CRC Crit. Rev. Biochem.* **1991**, *26*, 1.
3. Bhatt, N. P.; Patel, K.; Borchardt, R. T. *Pharm. Res.* **1990**, *7*, 793.
4. Geiger, T.; Clarke, S. *J. Biol. Chem.* **1987**, *262*, 785.
5. Stephenson, R. C.; Clarke, S. *J. Biol. Chem.* **1986**, *264*, 54.
6. Capasso, S.; Mazzarella, L.; Sica, F.; Zagon, A. *Peptide Res.* **1989**, *2*, 195.
7. (a) Bischoff, R.; Kolbe, V. J. H. *J. Chromatogr. B* **1994**, *662*, 261. (b) Bongers, J.; Heimer, E. P.; Lambros, T.; Pan, Y.; Campbell, R. M.; Felix, A. M. *Int. J. Peptide Protein Res.* **1992**, *36*, 364. (c) Artigues, A.; Farrant, H.; Schirch, V. *J. Biol. Chem.* **1993**, *268*, 13784.
8. (a) Gibbs, R. A.; Taylor, S. D.; Benkovic S. J. *Science* **1992**, *258*, 803. (b) Liotta, L. J.; Benkovic, P. A.; Miller, G. P.; Benkovic, S. J. *J. Am. Chem. Soc.* **1993**, *115*, 350.
9. Liotta, L. J.; Benkovic, P. A.; Miller, G. P.; Benkovic, S. J. *J. Am. Chem. Soc.* **1995**, *117*, 4729.
10. Kerrow, J. H.; Robinson, A. B. *Anal. Biol. Chem.* **1971**, *42*, 565.
11. Friedman, A. R.; Ichhpurani, A. K.; Brown, D. M.; Hillman, R. M.; Krabill, L. F.; Martin, R. A.; Zurcher-Neely, H. A.; Guido, D. M. *Int. J. Peptide Protein Res.* **1991**, *37*, 14.
12. Sun, A. Q.; Yuksel, K. U.; Rao, G. S. R.; Gracy, R. W. *Arch. Biochem. Biophys.* **1992**, *295*, 421.
13. Capasso, S.; Mazzarella, L.; Sica, F.; Zagari, A.; Salvatori, S. *J. Chem. Soc. Perkin. Trans.* **1993**, *2*, 679.
14. Capasso, S.; Mazzarella, L.; Kirby, A. J.; Salvatori, S. *Peptide Bond Cleavage* **1997**, 543.
15. Xu, M. Q.; Comb, D. G.; Paulus, H.; Noren, C. J.; Shao, Y.; Perler, F. *EMBO J.* **1994**, *13*, 5517.
16. Shao, C. J.; Xu, M. Q.; Paulus, H. *Biochemistry* **1995**, *34*, 10844.
17. Radkiewicz J. L.; Zipse H.; Clarke S.; Houk, K. N. *J. Am. Chem. Soc.* **1996**, *118*, 9148.
18. Frisch, M. J.; Trucks, G. W.; Schlegel, H. B.; Gill, P. M. W.; Johnson, B. G.; Robb, M. A.; Cheeseman, J. R.; Keith, T.; Petersson, G. A.; Montgomery, J. A.; Raghavachari, K.; Al-Laham, M. A.; Zakrzewski, V. G.; Ortiz, J. V.; Foresman, J. B.; Cioslowski, J.; Stefanov, B. B.; Nanayakkara, A.; Challacombe, M.; Peng, C. Y.; Ayala, P. Y.; Chen, W.; Wong, M. V.; Andres, J. L.; Repogle, E. S.; Gomperts, R.; Martin, R. L.; Fox, D. J.; Binkley, J. S.; Defrees, D. J.; Baker, J.; Stewart, J. J. P.; Head-Gordon, M.; Gonzales, C.; Pople, J. A.; *GAUSSIAN 94*, Revision C.3, Gaussian, Pittsburgh, PA, 1995.
19. Spartan Version 4.0, Wavefunction, Inc. 18401 Von Karman Ave., #370 Irvine, CA 92715, 1996.
20. Stewart, J. J. P. *J. Comput. Chem.* **1989**, *10*, 221.
21. Tomasi, J.; Miertus, S. *Chem. Phys.* **1982**, *65*, 239.
22. Lifson, S.; Hagler, A. T.; Dauger *J. Am. Chem. Soc.* **1979**, *101*, 5111.
23. Coll, M.; Frau, J.; Munoz, F.; Donoso, J. *J. Phys. Chem.* **1998**, *102*, 5915.
24. Kumar, G. A.; Pan, Y.; Smallwood, C. J.; McAllister, M. *J. Comput. Chem.* **1998**, *19*, 1345.
25. Wright, H. T. *Crit. Rev. Biochem. Mol. Biol.* **1991**, *26*, 1.